

# Reactive grasping using high-resolution tactile sensors

Reem Muhammed Al-Gaifi, Veit Müller and Norbert Elkmann\*

**Abstract**— This paper demonstrates the effectiveness of using high-resolution tactile sensors for a two-finger gripper for reactive grasping under conditions featuring uncertainty, whereas uncertainty will be understood as positioning inaccuracy induced by grasping planners and vision systems. Reactive grasping is defined here as the adoption of gripper pose in accordance to measured tactile sensor feedback. We propose a reactive grasping algorithm that in combination with high-resolution tactile sensors achieves grasping of unknown and novel objects with only one correction move. Extensive tests of the algorithm in different configurations showed a success rate of 91 % compared to 31 % without it.

## I. INTRODUCTION

A large challenge in the field of robotics when grasping novel objects is dealing with noisy and incomplete information, thus, sensory feedback during the grasp is of great importance for the early detection of failure and for performing the necessary adjustments to achieve an improved and more stable grasp [1]–[2]. Although vision systems are able to identify many properties of the objects to be grasped, their performance can be limited by environmental occlusion, lighting conditions, bad calibration, or imperfect control of the robot [3]. Inspired by humans, this uncertainty from the vision system can be compensated during grasp execution using haptic feedback. Haptic feedback using tactile sensors has received a lot of attention in research, whether it is during grasp execution such as haptic exploration [4]–[6], sensitive adaption of grasp configuration, the reactive grasping [7]–[9], or the post execution such as grasp stability assessment [10] and sensitive force adaptation whenever slip is being detected [11]–[18]. Although humans employ haptic exploration approaches to supplement any shortcomings from their sense of vision, in robotics this is often considered time consuming [19]. On the other hand, reactive grasping using haptic sensors usually employs the so called “haptic-glance” [20], which is a momentary haptic feedback used to obtain the initial information about the object status in-hand, after the initial object localization by an external system, e.g. vision system. Reactive grasping enables applying the necessary corrections on the robot to achieve a more stable grasp.

Reactive grasping algorithms address grasping under uncertainty. Hsiao *et al.* [3] developed and tested a tactile-sensing-based algorithm using a two-finger gripper to detect and react on the haptic contact during the grasp. It mainly identifies whether the contact between the object and the gripper was on the outer part of the finger, the inner part or a contact with the palm. If the contact was detected on the outer side of the finger, the robot moves up in the opposite direction. If the contact detected is in the inner area of the gripper, the



Figure 1. KUKA KR1100 sixx robot with Robotiq adaptive two-finger gripper with tactile sensors.

grasp is considered stable. If the contact is detected on the palm sensor, the grasp is considered impossible. According to Hyttinen *et al.* [1], the probability of a grasp success is computed and if the grasp is not stable, their algorithm performs a set of predefined actions while predicting the tactile data in each action and choosing the one with the highest probability to realize a stable grasp. The reactive grasping controller by Felip and Morales [7], evaluated with a three-finger gripper with tactile sensors and a force-torque sensor, corrects the position of the robot moving it in small iterations until the fingers are aligned with the object. Hasegawa *et al.* [14] use the tactile feedback from the sensor attached to a three-finger gripper to adjust the pose of each finger. This was done while attempting to take a book from a shelf. While re-grasping is beneficial to improve an unstable grasp, such multiple re-grasping trials to search for a stable grasp not only increase the time required for grasping a single object, compared to a direct grasp, but also unwillingly increase the possibility of moving the object during these attempts. This can negatively influence the success rate of grasping an object. Consequently, reducing the number of re-grasp trails would increase the efficiency of the grasping process. Hence, we present in this paper a tactile sensor based reactive grasping algorithm with a single re-grasp trial to adjust an unstable grasps. The algorithm is implemented with an adaptive two-finger gripper with high-resolution tactile sensors mounted on each fingertip and the re-grasp is achieved by calculating the correction distances after the first “haptic-glance”.

\*Authors are with Robotic Systems Business Unit, Fraunhofer Institute for Factory Operation and Automation IFF, 39106 Magdeburg, Germany (corresponding author, e-mail: reem.algaifi@iff.fraunhofer.de).

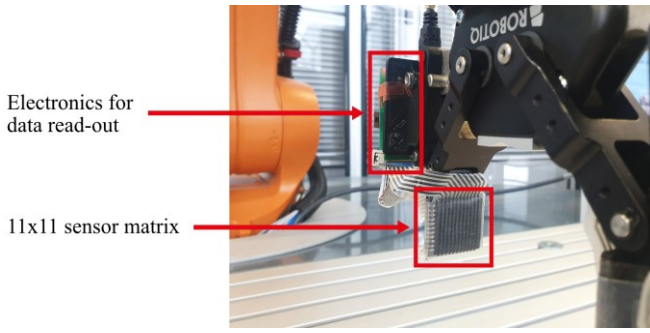


Figure 2. Piezoresistive tactile sensor with 2 mm spatial resolution attached to Robotiq gripper.

In the following, the hardware and platform used for this paper are explained. This is followed by an explanation of the reactive grasping algorithm. The experiment used to test the algorithm is then described, and the results are presented and discussed.

## II. HARDWARE AND PLATFORM

The gripper used in this experiment is an adaptive two-finger gripper from Robotiq with a grasp width of 85 mm. It is mounted on a KUKA KR10 R1100 sixx robot. The robot and the gripper unit are operated by ROS. The set-up is shown in Fig. 1.

The sensors main operating principle is based on the piezoresistive principle featuring the signal properties explained in [21]–[22]. For the given purpose, we designed compliant tactile sensors in an 11x11 sensor array, featuring a spatial resolution of 2 mm (Fig. 2). The data of each sensor matrix is updated at 50 Hz, which is needed to perform dynamical reactive grasping applications.

The tactile sensors used are tailor-made in size, shape and functionality, thereby allowing the sensors to optimally cope with all associated gripper requirements. The sensor design and integration follow a systematic approach, where the application context [23], working principle as well as size and shape of the grasping areas are taken into consideration. The sensors are attached to the fingertips of the Robotiq gripper and the electronics are mounted outside of the grasping area to prevent them from causing damage or other threatening harm during operation [21]. The updated tactile data is published by a ROS-node on a topic that is accessible by the reactive grasping algorithm at all times.

## III. REACTIVE GRASPING WITH TACTILE SENSORS

The tactile sensors attached to the fingers of the gripper detect contacts with an object and provide the first “haptic-glance”, due to the spatially resolved pressure feedback. The information about the grip is then fed forward to the controller that calculates the relative adaption of the gripper pose that increases the chance of achieving a stable grasp. The main idea is to align the sensor with the object while minimizing the number of correction moves.

It was assumed that a more stable grasp can be achieved during reactive grasping if the haptic feedback from the tactile sensors of both opposing sensors:

1. is equally distributed around the complete sensor face, or

2. is arranged around the center of the sensor, e.g. when the object is smaller than the grasping area of the gripper.

The tactile feedback of the high-resolution sensor provides information that can be used to localize the object in the grippers hold. Considering two opposing sensors with their corresponding sensor feedback in the gripper enables the calculation of the distance the robot has to move to achieve the conditions from these assumptions.

The reactive grasping component considers the following steps: The reactive grasping algorithm shown in Fig. 3 begins by removing the primarily pressure noise that is caused by a pre-strain, e.g. from a previous grasp. It then increases the grasping force gradually, closing the gripper, while checking for tactile sensor readings until contact on both fingers is detected. A predefined threshold is used to detect that contact has been made. This threshold is selected such that it is low enough to detect first contact with minimum possible grasp force and high enough to overcome possible sensor noise. After that, the tactile sensor data are analyzed to determine whether the grasp stability satisfies the stability assumption. If the algorithm detects an unstable grasp, a relative motion of the robot is executed in order to achieve a more stable grasp. Finally, the gripper closes with its maximum force regardless if the re-grasp led to an optimal grasp or not.

### A. Pre-filtering

The flexibility and the high resolution of our sensor comes at a price. During each grasp, the sensor reshapes according to

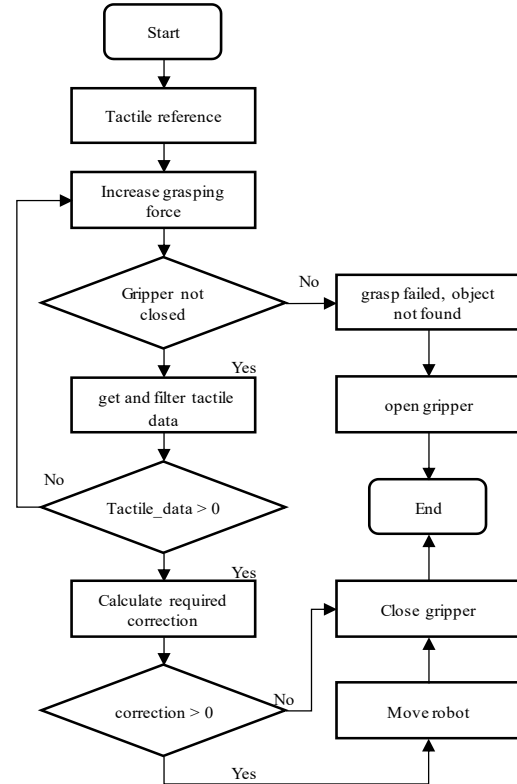


Figure 3. Reactive grasping algorithm for two-finger gripper whose fingers are covered with tactile sensors.

the object grasped. This can lead to false readings where no pressure is being applied, but tension is present. Therefore, different filters are applied to the acquired tactile data before further processing. The first filter removes the offset value that is, the data reading before the application of a force. Before each grasp attempt, the algorithm takes a reference reading of the tactile data and subtracts it from the new reading to ensure correct readings.

Then, a second filter is applied to remove unlikely data that result from a single faulty taxel. As the sensor has a high resolution, and since the objects in this experiment are larger than the sensors spatial resolution of 2 mm, it is very unlikely for a single taxel to have high readings while neighboring taxels do not. Therefore, we apply a box filter in the form of a 3x3 matrix that checks the neighboring taxels and sets any faulty taxel to zero.

### B. Re-grasp

The reactive grasping algorithm in this work compensates errors of the initial grasp pose in three dimensions: linear alignment (y-direction, z-direction), and angular orientation of  $\beta$  (Fig. 4). The linear position of x-direction and orientation of  $\alpha$  are neglected here, as they will be compensated by the closing of the gripper, i.e. when the gripper closes it will push the object in the appropriate direction. The angular position in  $\gamma$  is also neglected due to high risk of collisions with other objects, and because the error in this direction will be corrected as an error in z-direction.

#### 1) Corrections in z- and y-directions

For the linear corrections, each row of the tactile sensor data is averaged to provide a modeled column with the average of each row. The mean of the resulting column is calculated and used to divide these columns in order to remove taxels containing values less than the average. This results in values containing mainly the significant activated taxels, i.e. taxels in direct contact with the object, without the rows that are affected by indirect contact, i.e. non-active taxels. This leaves a column grid for the z-direction of 2 mm size, sensors spatial resolution, and a row grid by which the z-correction required can be calculated. Applying the calculated result should result in the pressure feedback to be equally distributed around the tactile sensors. The same principle is thereafter applied to calculate y but considering columns instead of rows and resulting in a row grid for the y-direction containing active and non-active cells (Fig. 5).

The correction in the y-direction is calculated by summing the non-active cells of the grid from the right and from the left and subtracting them from one another. This results in the



Figure 4. Axes used in reactive grasping with respect to robot from a flat table.

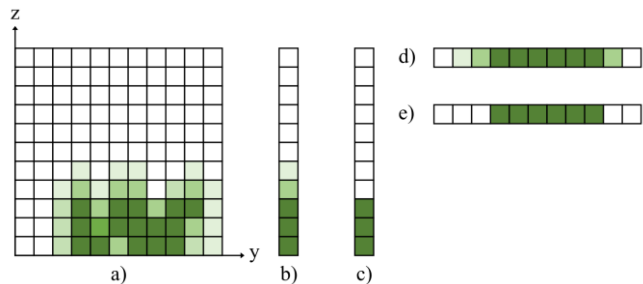


Figure 5. Illustration of the approach for correction measurements in z- and y-direction. a) Example of haptic feedback of a tactile sensor with 11x11 sensor cells. b) Line-wise averaged values of each row of the sensor matrix. c) Rows' average values after dividing by the mean. d) Line-wise averaged values of each active column of the sensor matrix. e) Columns' averaged values after dividing by the mean.

number of cells to shift the region of the activated cells in y-direction to the middle of the sensor, where the grasping stability assumptions are satisfied. This shift number is translated into distance in y-direction by multiplying it with the sensors' spatial resolution. The same approach is implemented for correction in z-direction.

#### 2) Corrections in $\beta$ -direction

After correct translational alignment, the column grids are evaluated with respect to the angular position  $\beta$  (Fig. 6). The contact points represent a right triangle when comparing the first activated cell of each column of both opposing sensors' feedback. The angular rotation required to align both opposing sensors is  $\beta$ . The geometrical parameter  $d$ , which is the distance between the two columns, is known. This is because the distance between the two fingers can be calculated from the gripper controller. The geometrical parameter  $l$  represents the number of non-active cells in the column grid multiplied by the sensors' spatial resolution. From basic geometry, the angle  $\beta$  can be calculated as follows:

$$\beta = \arctan (l/d)$$

Examples of re-grasping from unstable positions in y-, z- and  $\beta$ -direction are shown in Fig. 7.

## IV. EXPERIMENT

The robot is mounted on a table in a standard orientation, and objects to be gripped were placed on the table. The initial grasping poses are manually set and provided to the controller. The objects used in the experiment (see Table I) were chosen to cover a broad range of objects that are of different sizes, materials and weights. The sizes of the objects were limited to

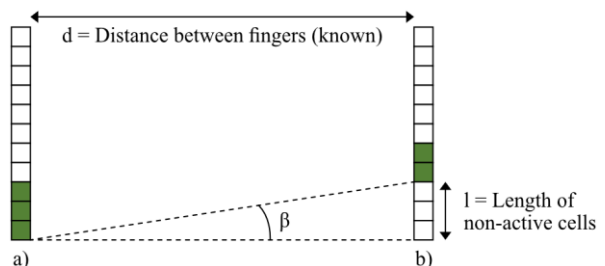


Figure 6. Illustration of the correction values in  $\beta$ -direction. a) Illustration of tactile data of left finger after averaging rows and dividing by mean. b) Illustration of tactile data of right finger after averaging rows and dividing by mean.

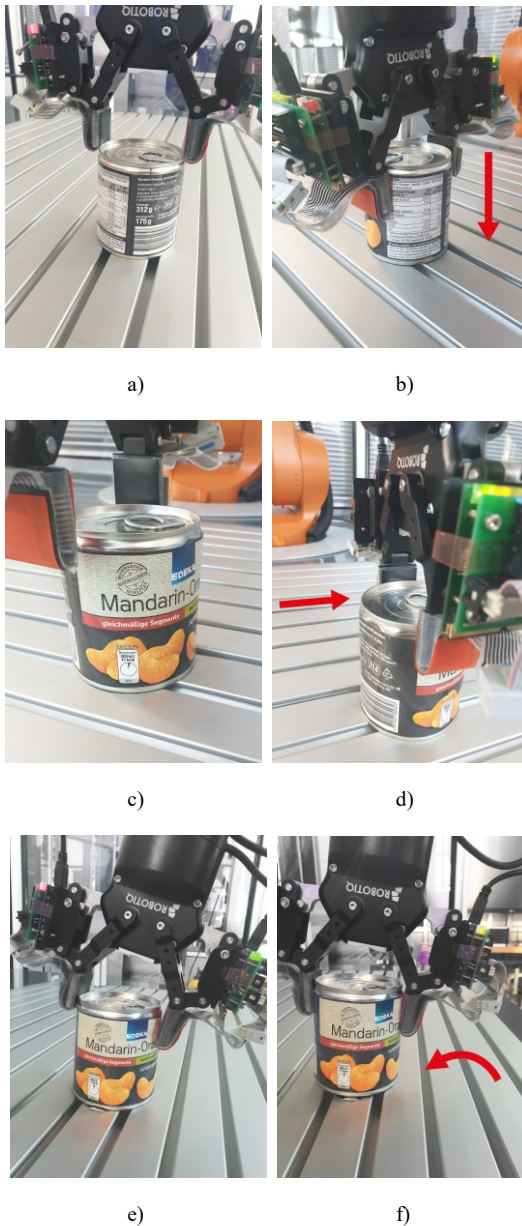


Figure 7. Reactive grasp examples in z-, y- and  $\beta$ -direction.

a) Haptic glance of object with unstable grasp. b) Re-grasp of object after correction in z direction. c) Haptic glance of object with unstable grasp. d) Re-grasp of object after correction in y direction. e) Haptic glance of object with unstable grasp. f) Re-grasp of object after correction in  $\beta$  direction.

those which are graspable by the Robotiq gripper. This means that objects must have a width less than 85 mm and height larger than 20 mm. For objects bigger than the 85 mm like o3 in Table I, the initial grasp pose is directed to the graspable portion of the object so that they fit inside the gripper.

For the evaluation of our algorithm attempts to grasp the objects with and without reactive grasping were executed. The grasp positions given to the controller were shifted from the optimal grasp positions to emulate pose estimation errors and testing how the algorithm can detect and fix them. Translation errors were tested in y-, z- and zy-axes, orientation errors in  $\beta$  as well as translation and orientation combination in  $y\beta$  (see Fig. 4). The translation errors were calculated with respect to how much the sensor area was covered by the objects to test

the limits of the algorithm. Positions where 10 %, 20 % and 30 % of the sensor area are covered by the object were tested as well as angles of 10, 20 and 30 degrees. The combination of  $z\beta$  and consequently  $yz\beta$  were not included as it was harder to keep the conditions of z-displacement in the presence of  $\beta$ -error in both fingers, i.e. to ensure that only 10 %, 20 % or 30 % of the sensors are in contact with the object. However, it was indirectly tested as the rotational error of  $\beta$  causes a displacement in z at least in one of the fingers.

The robot was commanded to the aforementioned positions and the grasps with and without reactive grasping capabilities were executed. The grasp with reactive grasping was performed following the algorithm in Fig. 3. The non-reactive grasping, on the other hand, was achieved by grasping the object with the maximum possible force of the gripper. After that, the object was lifted to a height of 200 mm and placed back on the table to ensure that the grasp was successful and the object was stable in the gripper. We also registered the correction values for the repeated tests objects o0 and o1 (see Table I) for the same configurations to compare the consistency of the algorithm's correction values.

TABLE I. REACTIVE GRASPING TEST OBJECTS

Different objects tested with reactive grasping using the two finger gripper with the red arrows showing the grasping points.

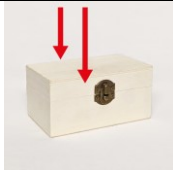
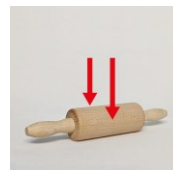
		
o0 wooden box	o1 plastic cylinder bottle	o2 paste like object with a plastic cover
		
o3 plastic spray object	o4 soft-plastic cylinder object	o5 plastic cylinder object
		
o6 glass bottle	o7 wooden rolling pin	o8 metal cylinder object
		
o9 metal object in a plastic bag		

TABLE II. REACTIVE GRASPING RESULTS

Results of grasping objects listed in Table I with predefined initial grasp positions and corresponding errors with reactive grasping. Results labeled “n/a” indicates that a particular grasp position does not satisfy the side size constraints of the gripper.

	o0	o1	o2	o3	o4	o5	o6	o7	o8	o9
z 10 %	5/5	5/5	5/5	5/5	0/2	2/2	2/2	2/2	5/5	2/2
z 20 %	5/5	5/5	5/5	5/5	0/2	2/2	2/2	2/2	5/5	2/2
z 30 %	5/5	5/5	5/5	4/5	0/2	2/2	2/2	2/2	5/5	2/2
y 10 %	5/5	4/5	2/2	n/a	0/2	2/2	2/2	2/2	5/5	n/a
y 20 %	5/5	5/5	2/2	n/a	0/2	2/2	2/2	2/2	5/5	n/a
y 30 %	5/5	5/5	2/2	n/a	0/2	2/2	2/2	2/2	5/5	n/a
yz 10 %	5/5	3/5	2/2	n/a	0/2	2/2	2/2	2/2	5/5	n/a
yz 20 %	5/5	5/5	2/2	n/a	0/2	2/2	2/2	2/2	5/5	n/a
yz 30 %	5/5	5/5	2/2	n/a	0/2	2/2	2/2	2/2	5/5	n/a
$\beta$ 10°	5/5	5/5	2/2	2/2	2/2	2/2	2/2	2/2	5/5	2/2
$\beta$ 20°	5/5	5/5	2/2	2/2	2/2	2/2	2/2	2/2	5/5	2/2
$\beta$ 30°	5/5	5/5	2/2	0/2	2/2	0/2	2/2	2/2	5/5	2/2
y $\beta$ 10	5/5	4/5	2/2	n/a	0/2	2/2	2/2	2/2	5/5	n/a
y $\beta$ 20	5/5	5/5	2/2	n/a	0/2	2/2	2/2	2/2	5/5	n/a
y $\beta$ 30	5/5	4/5	2/2	n/a	0/2	2/2	2/2	2/2	5/5	n/a

## V. RESULTS

The objects used were tested in 15 test configurations with and without reactive grasping. During the reactive grasping tests, the algorithm detected an unstable grasp after the first contact for all objects, and consequently, preformed a pose adjustment. The results of the tests are presented in Table II, while the results of direct grasps without reactive grasping can be found in Table III. The first row contains the names of the objects given in Table I, and the first column contains the errors with respect to how much of the sensor is covered for transitional errors and the degree of the error from a right grasp for the rotational error. A result of “n/a” in Table II and Table III indicates that in the particular grasp position contact in both fingers was not achievable.

A summary of the results is given in Table IV where the success rates are compared for each configuration. As can be seen in the table, our reactive grasping algorithm has an overall

TABLE III. NON-REACTIVE GRASPING RESULTS

Results of grasping objects listed in Table I with predefined initial grasp positions and corresponding errors without reactive grasping. Results labeled “n/a” indicates that a particular grasp position does not satisfy the side size constraints of the gripper.

	o0	o1	o2	o3	o4	o5	o6	o7	o8	o9
z 10 %	0/5	0/5	0/5	0/5	0/2	0/2	0/2	0/2	0/5	0/2
z 20 %	5/5	0/5	0/5	0/5	0/2	0/2	0/2	0/2	5/5	0/2
z 30 %	5/5	0/5	0/5	0/5	0/2	0/2	0/2	2/2	5/5	2/2
y 10 %	1/5	0/5	0/2	n/a	0/2	0/2	0/2	0/2	5/5	n/a
y 20 %	5/5	0/5	0/2	n/a	0/2	0/2	0/2	2/2	5/5	n/a
y 30 %	5/5	4/5	1/2	n/a	0/2	0/2	0/2	2/2	5/5	n/a
yz 10 %	0/5	0/5	0/2	n/a	0/2	0/2	0/2	0/2	0/5	n/a
yz 20 %	5/5	0/5	0/2	n/a	0/2	0/2	0/2	2/2	5/5	n/a
yz 30 %	5/5	0/5	0/2	n/a	0/2	0/2	0/2	2/2	5/5	n/a
$\beta$ 10°	5/5	5/5	0/2	2/2	0/2	0/2	0/2	2/2	5/5	2/2
$\beta$ 20°	0/5	5/5	0/2	0/2	0/2	0/2	0/2	2/2	5/5	0/2
$\beta$ 30°	0/5	5/5	0/2	0/2	0/2	0/2	0/2	0/2	0/5	0/2
y $\beta$ 10	0/5	0/5	0/2	n/a	0/2	0/2	0/2	0/2	5/5	n/a
y $\beta$ 20	0/5	0/5	0/2	n/a	0/2	0/2	0/2	2/2	0/5	n/a
y $\beta$ 30	0/5	0/5	0/2	n/a	0/2	0/2	0/2	2/2	0/5	n/a

TABLE IV. GRASPING RESULTS SUMMARY

Summary of grasping results with and without reactive grasping.

	non-reactive grasping	with reactive grasping
z 10 %	0/35 (0 %)	33/35 (94 %)
z 20 %	10/35 (29 %)	33/35 (94 %)
z 30 %	14/35 (40 %)	32/35 (91 %)
y 10 %	6/25 (24 %)	22/25 (88 %)
y 20 %	12/25 (48 %)	23/25 (92 %)
y 30 %	17/25 (68 %)	23/25 (92 %)
yz 10 %	0/25 (0 %)	21/25 (84 %)
yz 20 %	12/25 (48 %)	23/25 (92 %)
yz 30 %	12/25 (48 %)	23/25 (92 %)
$\beta$ 10 %	22/29 (76 %)	29/29 (100 %)
$\beta$ 20 %	12/29 (41 %)	29/29 (100 %)
$\beta$ 30 %	5/29 (17 %)	25/29 (93 %)
y $\beta$ 10%+10°	5/25 (20 %)	22/25 (88 %)
y $\beta$ 20%+20°	2/25 (8 %)	23/25 (92 %)
y $\beta$ 30%+30°	2/25 (8 %)	20/25 (88 %)
Total	131/417 (31 %)	381/417 (91 %)

success rate of 91 % for all tested objects compared to the non-reactive grasp, which only achieved 31 %.

The results of the registered correction values to evaluate the consistency of the corrections provided by the algorithm for the repeated tests of objects o0 and o1 in the same configuration are demonstrated in Fig. 8. The label “similar” includes results with the same values  $\pm 2$  mm or degrees for angles. The label “different” refers to results with a difference higher than  $\pm 2$  mm and “NONE” labels results where the direction of the error was not corrected.

## VI. DISCUSSION

Table IV clearly shows a great improvement of grasping objects with the proposed reactive grasping algorithm to achieve a stable grasp with only one correction move. Although the errors of our configurations were calculated with respect to the sensor, it was not that far off from the center of the objects, which is usually the position acquired from vision systems, of cylindrical form like o1 and o4 in z-direction as well as o5 and o8 in y-direction. The algorithm shows a great success regardless of the different shapes, edges and corners. Object o4, which has shown to be the object with the lowest grasp success rate, has a high weight and a slippery surface, as it is smooth plastic filled with liquid. During its

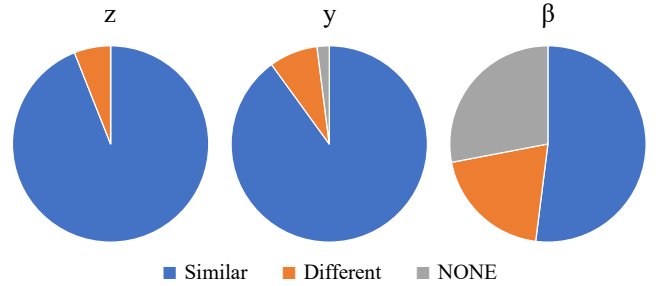


Figure 8. Reactive grasping algorithm results for z-, y- and  $\beta$ -corrections values. In this figure, “similar” labels correction values of the same amount or with 2 mm or 2° difference. “Different” labels values with difference greater than 2 mm or 2° and “NONE” means the direction of the error was not corrected.

grasp with this algorithm, the object was detected, the grasp was corrected and the fingers were covered completely, but the grasp failed during the lifting sequence of the grasp.

Fig. 8 shows that the results of in z- and y-direction were consistent in most of the cases. Results for  $\beta$  differed, as sometimes the angle error was not detected and a compensation in the z-direction was calculated instead. This could be due to the shape of the object that limits the contact in the middle of the sensor, resulting in an angle calculation. Another reason could be noise in the tactile data that was not removed despite the filtering.

A possible improvement for the algorithm is the detection of stability of the objects. Since we consider grasps where the object is not completely covering the sensor, unstable corrections are executed although a direct grasp could have achieved a stable grasp. This could be time-consuming in a bin-picking scenario. We believe that the use of deep learning to detect stability of grasp could solve this problem [10].

## VII. CONCLUSION

In this paper, we presented a model-based reactive grasping algorithm that utilizes high-resolution tactile sensors of 2 mm spatial resolution to correct an unstable grasp. The experimental results with objects of different shapes and elastic properties demonstrated a significant improvement in the success and stability of grasp planning with a two-finger gripper. This was achieved through the enlargement of the initial partial contact area of the fingertips of the gripper with the object. It showed a success rate of 91 % with only one move of correction compared to 31 % success rate for the same objects and grasp positions without reactive grasping.

## ACKNOWLEDGMENT

This paper describes research carried out at Fraunhofer Institute for Factory Operation and Automation IFF, Magdeburg. The research leading to these results has been supported by the PICKLACE project. The PICKLACE project is being funded by the EU's Horizon 2020 research and innovation program under grant agreement number 780488.

## REFERENCES

- [1] E. Hyttinen, D. Kragic, and R. Detry, Eds., "Estimating tactile data for adaptive grasping of novel objects," in *2017 IEEE-RAS 17th Int. Conf. Humanoid Robotics (Humanoids)*, Birmingham, 2017, pp. 643–648, doi: [10.1109/HUMANOIDS.2017.8246940](https://doi.org/10.1109/HUMANOIDS.2017.8246940).
- [2] Y. Chebotar, K. Hausman, Z. Su, G. S. Sukhatme, and S. Schaal, "Self-supervised regrasping using spatio-temporal tactile features and reinforcement learning," in *2016 IEEE/RSJ Int. Conf. Intelligent Robots and Systems (IROS)*, Daejeon, South Korea, 2016, pp. 1960–1966, doi: [10.1109/IROS.2016.7759309](https://doi.org/10.1109/IROS.2016.7759309).
- [3] K. Hsiao, S. Chitta, M. Ciocarlie, and E. Gil Jones, Eds., "Contact-reactive grasping of objects with partial shape information," in *2010 IEEE/RSJ Int. Conf. Intelligent Robots and Systems*, Taipei, 2010, pp. 1228–1235, doi: [10.1109/IROS.2010.5649494](https://doi.org/10.1109/IROS.2010.5649494).
- [4] Lorenzo Natale and Eduardo Torres-jara, Ed., "A sensitive approach to grasping," in *Proc. 6th Int. Workshop Epigenetic Robotics*, 2006.
- [5] J. Felip, J. Bernabé, and A. Morales, Eds., "Contact-based blind grasping of unknown objects," in *2012 12th IEEE-RAS Int. Conf. Humanoid Robots (Humanoids 2012)*, Osaka, 2012, pp. 396–401, doi: [10.1109/HUMANOIDS.2012.6651550](https://doi.org/10.1109/HUMANOIDS.2012.6651550).
- [6] S. C. Abdullah, J. Wada, M. Ohka, and H. Yusoff, Eds., "Object Exploration Algorithm Based on Three-Axis Tactile Data," in *2010 4th Asia Int. Conf. Mathematical/Analytical Modelling and Computer Simulation*, Bornea, 2010, pp. 158–163, doi: [10.1109/AMS.2010.43](https://doi.org/10.1109/AMS.2010.43).
- [7] J. Felip and A. Morales, Eds., "Robust sensor-based grasp primitive for a three-finger robot hand," in *2009 IEEE/RSJ Int. Conf. Intelligent Robots and Systems*, St. Louis, MO, 2009, pp. 1811–1816, doi: [10.1109/IROS.2009.5354760](https://doi.org/10.1109/IROS.2009.5354760).
- [8] K. Hsiao, P. Nangeroni, M. Huber, A. Saxena, and A. Ng, "Reactive Grasping Using Optical Proximity Sensors," in *2009 IEEE Int. Conf. Robotics and Automation*, Kobe, 2009, pp. 2098–2105, doi: [10.1109/ROBOT.2009.5152849](https://doi.org/10.1109/ROBOT.2009.5152849).
- [9] Wu, Bohan, Ireteayo Akinola, Jacob Varley and Peter Allen. "MAT: Multi-Fingered Adaptive Tactile Grasping via Deep Reinforcement Learning." CoRL (2019).
- [10] Y. Bekiroglu, J. Laaksonen, J. A. Jorgensen, V. Kyrki, and D. Kragic, "Assessing Grasp Stability Based on Learning and Haptic Data," *IEEE Trans. Robot.*, vol. 27, no. 3, pp. 616–629, Jun. 2011, doi: [10.1109/TRO.2011.2132870](https://doi.org/10.1109/TRO.2011.2132870).
- [11] Z. Ding, N. Paperno, K. Prakash and A. Behal, "An Adaptive Control-Based Approach for 1-Click Gripping of Novel Objects Using a Robotic Manipulator," in *IEEE Transactions on Control Systems Technology*, vol. 27, no. 4, pp. 1805–1812, Jul. 2019, doi: [10.1109/TCST.2018.2821651](https://doi.org/10.1109/TCST.2018.2821651).
- [12] J. Venter and A. M. Mazid, "Tactile sensor based intelligent grasping system," in *2017 IEEE Int. Conf. Mechatronics (ICM)*, Churchill, Australia, 2017, pp. 303–308, doi: [10.1109/ICMECH.2017.7921121](https://doi.org/10.1109/ICMECH.2017.7921121).
- [13] M. Al-Mohammed, Z. Ding, P. Liu, and A. Behal, "An Adaptive Control Based Approach for Gripping Novel Objects with Minimal Grasping Force," in *2018 IEEE 14th Int. Conf. Control and Automation (ICCA)*, Anchorage, AK, 2018, pp. 1040–1045, doi: [10.1109/ICCA.2018.8444179](https://doi.org/10.1109/ICCA.2018.8444179).
- [14] H. Hasegawa, Y. Mizoguchi, K. Tadakuma, A. Ming, M. Ishikawa and M. Shimojo, "Development of intelligent robot hand using proximity, contact and slip sensing," in *2010 IEEE Int. Conf. Robotics and Automation*, Anchorage, AK, 2010, pp. 777–784, doi: [10.1109/ROBOT.2010.5509243](https://doi.org/10.1109/ROBOT.2010.5509243).
- [15] D. Gunji, T. Araki, A. Namiki, A. Ming, and M. Shimojo, "Grasping Force Control of Multi-fingered Robot Hand based on Slip Detection Using Tactile Sensor," *J. Robotics Society Japan*, vol. 25, no. 6, pp. 970–978, Jan. 2007, doi: [10.7210/jrsj.25.970](https://doi.org/10.7210/jrsj.25.970).
- [16] E. D. Engeberg and S. G. Meek, "Adaptive Sliding Mode Control for Prosthetic Hands to Simultaneously Prevent Slip and Minimize Deformation of Grasped Objects," in *IEEE/ASME Trans. Mechatron.*, vol. 18, no. 1, pp. 376–385, Feb. 2013, doi: [10.1109/TMECH.2011.2179061](https://doi.org/10.1109/TMECH.2011.2179061).
- [17] S. Teshigawara, M. Ishikawa and M. Shimojo, "Development of high speed and high sensitivity slip sensor," in *2008 IEEE/RSJ Int. Conf. Intelligent Robots and Systems*, Nice, 2008, pp. 47–52, doi: [10.1109/IROS.2008.4650688](https://doi.org/10.1109/IROS.2008.4650688).
- [18] M. Stachowsky, T. Hummel, M. Moussa, and H. A. Abdullah, "A Slip Detection and Correction Strategy for Precision Robot Grasping," in *IEEE/ASME Trans. Mechatron.*, vol. 21, no. 5, pp. 2214–2226, Oct. 2016, doi: [10.1109/TMECH.2016.2551557](https://doi.org/10.1109/TMECH.2016.2551557).
- [19] A. J. Spiers, M. V. Liarokapis, B. Calli, and A. M. Dollar, "Single-Grasp Object Classification and Feature Extraction with Simple Robot Hands and Tactile Sensors," in *IEEE Transactions on Haptics*, vol. 9, no. 2, pp. 207–220, Apr.–Jun. 2016, doi: [10.1109/TOH.2016.2521378](https://doi.org/10.1109/TOH.2016.2521378).
- [20] R. L. Klatzky and S. J. Lederman, "Identifying objects from a haptic glance," *Perception & Psychophysics*, vol. 57, no. 8, pp. 1111–1123, Nov. 1995, doi: [10.3758/BF03208368](https://doi.org/10.3758/BF03208368).
- [21] V. Müller, T. Lam and N. Elkmann, "Sensor design and model-based tactile feature recognition," in *2017 IEEE SENSORS*, Glasgow, 2017, pp. 1–3, doi: [10.1109/ICSENS.2017.8234169](https://doi.org/10.1109/ICSENS.2017.8234169).
- [22] V. Müller, M. Fritzsche and N. Elkmann, "Sensor design and calibration of piezoresistive composite material," in *2015 IEEE SENSORS*, Busan, 2015, pp. 1–4, doi: [10.1109/ICSENS.2015.7370488](https://doi.org/10.1109/ICSENS.2015.7370488).
- [23] V. Mueller, C. Urbahn, R. M. Al-Gaifi, M. Schmidt, J. Saenz and N. Elkmann, "Tactile Sensor Modules for Flexible Manipulation," in *ISR 2018: 50th Int. Symp. Robotics*, Munich, Germany, Jun. 2018, pp. 1–7.